

# Radiogenic Neutron Background

v2.1

J. Cooley,<sup>3</sup> D.-M. Mei,<sup>4</sup> K.J. Palladino,<sup>2</sup> H. Qiu,<sup>3</sup> M. Selvi,<sup>1</sup> S. Scorza,<sup>3,5</sup> C. Zhang,<sup>4</sup> and ....

(The AARM Collaboration)

<sup>1</sup>*INFN - Sezione di Bologna, Italy*

<sup>2</sup>*Department of Physics, University of Wisconsin-Madison, Madison, WI 53706, USA*

<sup>3</sup>*Department of Physics, Southern Methodist University, Dallas, TX 75275, USA*

<sup>4</sup>*Department of Physics, University of South Dakota, Vermillion, USA*

<sup>5</sup>*Karlsruhe Institute of Technology, Institute of Experimental Nuclear Physics, Gaedestr. 1, 76128 Karlsruhe, Germany*

(Dated: February 23, 2016)

Ultra-low-background experiments, generically termed rare-event searches, address some of the most important open questions in particle physics, cosmology and astrophysics: direct detection of dark matter, neutrinoless double beta decay, proton decay, and detection of solar and supernovae neutrinos. Although their detection methods and physics goals are varied, rare-event searches share a number of common requirements in order to obtain sensitivity to low-rate processes in the presence of an overwhelming rate of environmental radiation, including the need for significant rock overburdens to moderate the flux of cosmic-ray muons. This requirement is so universal that an international community of underground science has emerged, with dozens of experiments operating in mines that vary in depth from a few hundred to many thousand meters water equivalent (m.w.e.) .

Simulations are used to understand backgrounds caused by naturally occurring radioactivity in the rock and in every piece of shielding and detector material used in the experiment. Most important are processes like spontaneous fission and ( $\alpha$ ,n) reactions in material close to the detectors that can produce neutrons. A comparison study between two dedicated softwares is detailed. Neutron yields and spectra obtained with Mei-Zhang-Hime and SOURCES4 codes are presented.

## I. INTRODUCTION

Reduction of radiogenic backgrounds is one of the most important factors for rare event search experiments including searches for dark matter and neutrino-less double beta decay. These radiogenic backgrounds can be generically classified into two types: electron recoil and nuclear recoil backgrounds. Electron recoil background result from the interactions of gamma rays, electrons or beta particles interacting with the electrons in the detector's target medium while nuclear recoil backgrounds result from neutrons interacting with the nucleus in the detector's target medium. In dark matter experiments, the nuclear recoil background is of particular concern because a nuclear recoil from a neutron can be indistinguishable from a nuclear recoil from a WIMP.

Neutrons are produced by spontaneous fission,  $\alpha$ -n interactions and muon-induced interactions. Muon-induced neutrons can be reduced by operation the detector deep underground and by placing passive shielding around the detector. In addition, muon-induced neutrons can often be recognized by identifying the parent muon in a muon veto. More difficult to deal with are neutrons resulting from  $\alpha$ -n interactions and spontaneous fission from <sup>238</sup>U, <sup>235</sup>U, and <sup>232</sup>Th present in the materials used to construct the shielding and the detectors themselves. Thus, experimentalists must select their materials carefully when designing and constructing their experiments. This requires that they have accurate simulations of the processes in the materials they are considering.

There are currently two codes available for use in such calculations, SOURCES-4 [1] and a second code devel-

oped by Mei, Zhang and Hei [2] which we will refer to as the USD code.

## II. NEUTRON YIELD AND SPECTRA

The measurements of neutron spectra strongly depend on the material and are not straightforward since neutrons are neutral particles. Their calculations are critical for low background experiments. The total neutron yield indicates the number of neutrons which are produced or had entered the target whereas the neutron energy spectrum determines the background events we would expect in the energy range of interest. Both are needed in order to carry out a complete and reliable neutron background simulation. The evaluation of neutron yields and spectra can be performed via different codes: the modified version of SOURCES4A and the code developed by Mei, Zhang and Hime made available online at <http://neutronyield.usd.edu> have been considered. SOURCES4 code has been modified to extend the cross section for ( $\alpha$ ,n) up to 10 MeV, based on experimental data, whenever possible, and calculations performed via the EMPIRE code [3] by the group at the University of Sheffield. The SOURCES4A and USD codes calculate neutron yields and spectra from ( $\alpha$ , n) reactions due to the decay of radionuclides. Radiogenic neutrons result from the decay of the intrinsic contamination of materials surrounding the detectors with <sup>232</sup>Th, <sup>238</sup>U and <sup>235</sup>U. A comparison study between SOURCES4 and USD codes is carried out considering the <sup>232</sup>Th and the <sup>238</sup>U decay chains in secular equilibrium, although a possibility

85 of disequilibrium can be taken into account: due to mi-  
86 gration differently, the long-lived isotopes,  $^{226}\text{Ra}$ ,  $^{222}\text{Rn}$ ,  
87  $^{210}\text{Po}$ ,  $^{228}\text{Ra}$ ,  $^{228}\text{Th}$  and the associated decay daugh-  
88 ters could be calculated separately, see table I. For both  
89 chains, most of the neutrons are produced by the  $\alpha$  gen-  
90 erated in the second part of the chains.

TABLE I. Radiogenic neutron yield ( $\text{n}\cdot\text{s}^{-1}\cdot\text{cm}^{-3}$ ) from ( $\alpha$ , n) reactions in different materials for 1ppb of  $^{238}\text{U}$  and  $^{232}\text{Th}$  decay chains. Neutron yield have been calculated via the modified SOURCES4A code.

Material	Neutron yield for 1ppb ( $\text{n}\cdot\text{s}^{-1}\cdot\text{cm}^{-3}$ )	
	$^{238}\text{U} \rightarrow ^{226}\text{Ra}$	$^{226}\text{Ra} \rightarrow ^{206}\text{Pb}$
Stainless Steel	$6.4 \cdot 10^{-15}$	$3.1 \cdot 10^{-11}$
Pyrex	$4.0 \cdot 10^{-11}$	$1.9 \cdot 10^{-10}$
Borosilicate Glass	$6.3 \cdot 10^{-11}$	$2.8 \cdot 10^{-10}$
Titanium	$1.14 \cdot 10^{-13}$	$1.0 \cdot 10^{-10}$
Copper	$0.0 \cdot 10^{-11}$	$2.8 \cdot 10^{-12}$
PE ( $\text{C}_2\text{H}_4$ )	$1.6 \cdot 10^{-12}$	$1.1 \cdot 10^{-11}$
PTFE ( $\text{CF}_2$ )	$1.8 \cdot 10^{-10}$	$1.6 \cdot 10^{-9}$
	$^{232}\text{Th} \rightarrow ^{228}\text{Th}$	$^{228}\text{Th} \rightarrow ^{208}\text{Pb}$
Stainless Steel	$8.8 \cdot 10^{-19}$	$4.1 \cdot 10^{-11}$
Pyrex	$2.4 \cdot 10^{-12}$	$8.4 \cdot 10^{-11}$
Borosilicate Glass	$3.8 \cdot 10^{-12}$	$1.2 \cdot 10^{-10}$
Titanium	$4.4 \cdot 10^{-16}$	$9.3 \cdot 10^{-11}$
Copper	$0.0 \cdot 10^{-11}$	$9.5 \cdot 10^{-12}$
PE ( $\text{C}_2\text{H}_4$ )	$1.6 \cdot 10^{-13}$	$5.1 \cdot 10^{-12}$
PTFE ( $\text{CF}_2$ )	$7.1 \cdot 10^{-12}$	$7.7 \cdot 10^{-10}$

91  
92  
93 The calculation of the neutron spectra requires as in-  
94 put the cross-sections of ( $\alpha$ , n) reactions, the probabilities  
95 of nuclear transition to different excited states (branch-  
96 ing ratio) and the alpha emission lines from the radioac-  
97 tive radionuclides. Both codes consider a thick target:  
98 calculation of neutron yields and spectra are carried out  
99 under the assumption that the size of radioactive sam-  
100 ple exceeds significantly the range of the alpha particle.  
101 The energy bin size of the ( $\alpha$ , n) calculation is fixed  
102 to be 0.1 MeV in USD code while is user dependent in  
103 SOURCES4A.

104 Table II lists the  $\alpha$ -lines respectively resulting from  
105 the  $^{232}\text{Th}$  and  $^{238}\text{U}$  decay chains that are present in  
106 SOURCES4A and USD codes. USD code is missing the  
107  $\alpha$ -lines from the  $^{222}\text{Ra}$  isotope in the  $^{238}\text{U}$  decay chain  
108 that is considered by the SOURCES4A library. Over-  
109 all, the branching ratio and the energy lines are in good  
110 agreement between the two codes.

111 Cross-sections and branching ratios are required as well  
112 for neutron yield and spectra calculations. The USD  
113 code uses TENDL 2012 [4] to provide ( $\alpha$ , n) nuclear  
114 cross-sections. TENDL is a validated nuclear data li-  
115 brary which provides the output of the TALYS [5] nu-  
116 clear model code system; the SOURCES4 cross section  
117 input libraries come from EMPIRE2.19 [3] calculations  
118 and, for some isotopes, a combination of data measure-  
119 ments and EMPIRE2.19 calculations. Also, EMPIRE is  
120 the code recommended by International Atomic Energy  
121 Agency (IAEA). Neither EMPIRE nor TALYS can cal-

TABLE II. Alpha lines present in SOURCES4A and USD, and their intensity (BR) for isotopes in the  $^{232}\text{Th}$  and  $^{238}\text{U}$  decay chains. Only lines with intensity  $> 1\%$  have been quoted.

Isotopes	SOURCES4A		USD	
	Line (keV)	BR (%)	Line (MeV)	BR (%)
$^{238}\text{U}$	4151	21	4.151	21
	4198	79	4.198	79
$^{234}\text{U}$	4722.4	28.42	4.722	28.6
	4774.6	71.38	4.775	71.4
$^{230}\text{Th}$	4620.5	23.4	4.621	23.7
	4687.0	76.3	4.688	76.3
$^{226}\text{Ra}$	4601	5.55	4.602	5.6
	4784.34	94.45	4.784	94.4
$^{222}\text{Rn}$	5489	99.92	5.490	100
$^{218}\text{Po}$	6002.35	99.98	6.002	100
$^{214}\text{Po}$	7686.82	99.99	7.687	99.99
$^{210}\text{Po}$	5304.33	99.99	5.304	100
$^{232}\text{Th}$	3947.2	21.7	3.954	22.1
	4012.3	78.2	4.013	77.9
$^{228}\text{Th}$	5340.36	27.2	5.340	28.5
	5423.15	72.2	5.423	71.5
$^{224}\text{Ra}$	5448.6	5.06	5.449	5.1
	5685.37	94.92	5.685	94.9
$^{220}\text{Rn}$	6288.3	99.99	6.288	100
$^{216}\text{Po}$	6778.5	99.99	6.778	100
$^{212}\text{Bi}$	6051.1	25.16	6.050	26.2
	6090.2	9.79	6.0902	9.8
$^{212}\text{Po}$	8784.6	100	8.784	64

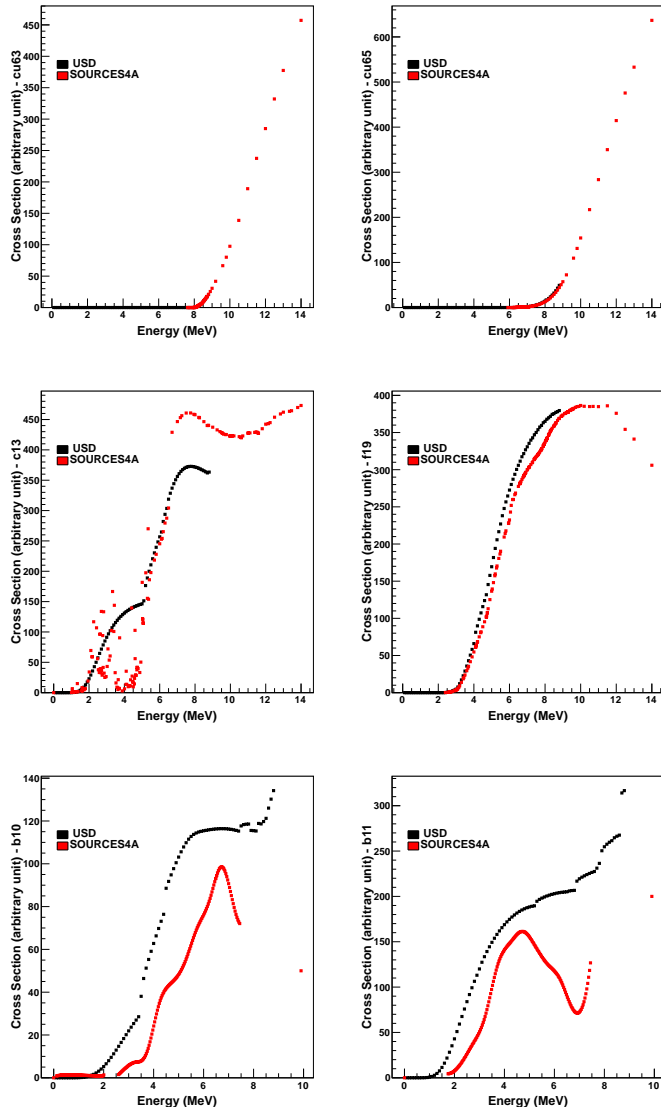
TABLE III. Radiogenic neutron yield ( $\text{n}/\text{s}/\text{cm}^3$ ) for copper and polyethylene materials and for  $^{238}\text{U}$  and  $^{232}\text{Th}$  decay chains. Column (1) and (2) refer to pure USD and SOURCES4A calculation, respectively. Column (3) refers to SOURCES4A calculation with USD ( $\alpha$ , n) cross section libraries. A ratio of the neutron yield is also provided: column (a) refers to the ratio of (2) over (1), whereas column (b) corresponds to the ratio (2)/(3)

Material	Chain	Neutron Yield ( $10^{-12} \cdot \text{n}\cdot\text{s}^{-1}\cdot\text{cm}^{-3}$ )			Ratio	
		(1)	(2)	(3)	(a)	(b)
Copper	$^{238}\text{U}$	3.46	2.84	2.93	0.8	1.0
	$^{232}\text{Th}$	11.1	9.49	9.18	0.9	1.0
Polyethylene ( $\text{C}_2\text{H}_4$ )	$^{238}\text{U}$	9.56	12.6	16.4	1.3	0.8
	$^{232}\text{Th}$	2.87	5.28	5.97	1.8	0.9

122 culate properly resonance behavior which has been ex-  
123 perimentally observed.

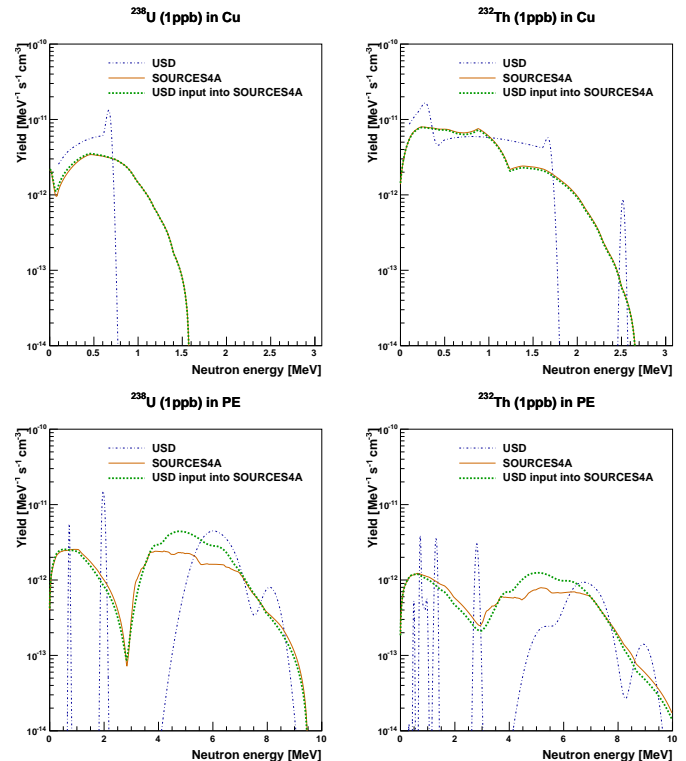
124 An extensive comparison between the different cross-  
125 section libraries used in USD and SOURCES4A has been  
126 carried out for the target nuclides present in the mate-  
127 rials contributing the most to radiogenic neutron back-  
128 ground. Specifically, we refer to materials which com-  
129 pose the shielding scheme and the internal detector parts,  
130 such as stainless steel, copper, titanium, borosilicate glass  
131 (PMTs glass), PTFE which become important when the  
132 external flux is attenuated by the shielding. Comparison  
133 of cross section inputs results in a good agreement for  
134

FIG. 1. Input ( $\alpha, n$ ) cross-section for the target isotopes involved in radiogenic neutron calculations for copper and polyethylene. Red markers refers to SOURCES4A inputs, whereas the black markers to USD. From left to right, top to bottom:  $^{63}\text{Cu}$ ,  $^{65}\text{Cu}$ ,  $^{13}\text{C}$ ,  $^{19}\text{F}$ ,  $^{10}\text{B}$  and  $^{11}\text{B}$ .



most of isotopes in both code libraries. For some, such as  $^{13}\text{C}$  and  $^{10}\text{B}$  and  $^{11}\text{B}$  the cross sections show discrepancies. To better understand the contribution due to the cross section input library in the radiogenic neutron yield and spectra we have calculated radiogenic neutron yield and spectra for two different materials: copper, for which the input cross sections in both codes are matching, and polyethylene, for which input cross sections of  $^{13}\text{C}$  show discrepancies between the codes, details in figure 1. We have considered natural copper (70%  $^{63}\text{Cu}$  and 30%  $^{65}\text{Cu}$ ) with a density of 8.96 g/cm<sup>3</sup>; polyethylene material (C<sub>2</sub>H<sub>4</sub>) is considered with a density

FIG. 2. Radiogenic neutron spectra ( $\text{n}\cdot\text{MeV}^{-1}\cdot\text{s}^{-1}\cdot\text{cm}^{-3}$ ) calculated for 1ppb  $^{238}\text{U}$  and  $^{232}\text{Th}$  decay chains, left and right panels, respectively. First row show copper contribution, lower row polyethylene material. Dotted blu lines refers to pure USD calculations, plain orange line to pure SOURCES4A calculations and dashed green line is the mixed computation for which we ran SOURCES4A algorithm with input cross section of USD code.



of density is 0.935 g/cm<sup>3</sup>. Estimates are done for 1ppb in  $^{238}\text{U}$  and  $^{232}\text{Th}$  decay chains. Calculations consist of pure SOURCES4A and USD computation and a mixed computation for which we run SOURCES4A algorithm with cross section inputs of USD. Resulting radiogenic neutron yields are quoted in table III. The column (a) of the radiogenic neutron yield ratio quotes the calculation differences between SOURCES4A and USD codes: they show a reasonably good agreement, inside a 50% discrepancy. The column (b) refers to the ratio of radiogenic neutron yield resulting from the same algorithm calculation (SOURCES4A) but with USD (column (3)) and SOURCES4A (column (2)) input ( $\alpha, n$ ) cross-sections. For polyethylene, we can conclude that the input cross-section may account up to a 20% discrepancy in neutron yield. Figure 3 shows radiogenic neutron spectra for copper (upper row) and polyethylene (lower row), both from uranium and thorium decay chains, left and right panels respectively.

A comparison of neutron yield and energy spectrum obtained via SOURCES4A and USD codes for different material has been carried out. Results are shown in ta-

ble IV and figure 3. A qualitative agreement between the two codes is observed. A maximum discrepancy of a factor 2 is found. The energy spectra calculated via SOURCES4A code are in general smoother, without the presence of peaks, feature of USD spectra.

TABLE IV. Radiogenic neutron yield ( $\text{n}\cdot\text{s}^{-1}\cdot\text{cm}^{-3}$ ) per material considering 1ppb of  $^{238}\text{U}$  and  $^{232}\text{Th}$ . The percentage difference is calculated as  $(\text{SOURCES4A}-\text{USD})/[(\text{SOURCES4A}+\text{USD})/2]$ .

Material	Chain	Neutron Yield ( $\text{n}\cdot\text{s}^{-1}\cdot\text{cm}^{-3}$ )		Diff %
		SOURCES4A	USD	
Cu	$^{238}\text{U}$	2.84E-12	3.46E-12	20
	$^{232}\text{Th}$	9.49E-12	1.11E-11	16
PE ( $\text{CH}_2$ )	$^{238}\text{U}$	1.26E-11	9.56E-12	-27
	$^{232}\text{Th}$	5.28E-12	2.87E-12	-59
Titanium	$^{238}\text{U}$	$1.04 \cdot 10^{-10}$	$1.99 \cdot 10^{-10}$	-63
	$^{232}\text{Th}$	$9.29 \cdot 10^{-11}$	$1.24 \cdot 10^{-10}$	-28
Stainless Steel	$^{238}\text{U}$	$3.10 \cdot 10^{-11}$	$5.95 \cdot 10^{-11}$	-63
	$^{232}\text{Th}$	$4.05 \cdot 10^{-11}$	$6.80 \cdot 10^{-11}$	-51
Pyrex	$^{238}\text{U}$	$2.30 \cdot 10^{-10}$	$1.61 \cdot 10^{-10}$	36
	$^{232}\text{Th}$	$8.66 \cdot 10^{-11}$	$4.59 \cdot 10^{-11}$	61
Borosilicate Glass	$^{238}\text{U}$	$3.48 \cdot 10^{-10}$	$2.45 \cdot 10^{-10}$	35
	$^{232}\text{Th}$	$1.27 \cdot 10^{-10}$	$6.98 \cdot 10^{-11}$	58
PTFE ( $\text{CF}_2$ )	$^{238}\text{U}$	$1.81 \cdot 10^{-9}$	$1.60 \cdot 10^{-9}$	12
	$^{232}\text{Th}$	$7.76 \cdot 10^{-10}$	$5.42 \cdot 10^{-10}$	36

### III. GEANT4 PROPAGATION

To evaluate the impact of the varying neutron spectra produced by SOURCES4A and the USD calculator, simplified detector geometries were created within a RAT [6] framework with Geant4.9.5.p01 and the pertinent high precision neutron physics list utilizing cross sections from G4NDL3.14 for neutrons under 20 MeV. Four simulations, for neutrons from uranium and thorium, with the spectra from SOURCES4A and USD (shown in Figure /reffig:ratspectra) were run for each relevant material under study.

Three simplified direct dark matter detector geometries were established to study neutron elastic scatter signals within central detector materials and the potential for vetoing neutrons with outer detectors. The first was a spherical liquid argon detector, with a radius of 1 m, is surrounded by shells of 10 cm thick acrylic, 5 mm thick borosilicate glass, and a water veto out to a radius of 3 m. The simulated neutrons were isotropically created in the borosilicate glass, as it is the leading source of radiogenic neutrons in many liquid argon detectors.

The second geometry studied was a cylindrical liquid xenon detector with a 1 m diameter and height. It is nested within cylinders of 3 cm thick PTFE, 2 cm thick titanium, and liquid scintillator veto with a diameter and

height of 3 m. Neutrons were generated isotropically in the PTFE for variety of materials studied; it is not likely to be the leading source of neutron backgrounds for most xenon detectors.

The final geometry studied was a cylindrical solid germanium detector with a 10 cm diameter and 120 cm height. It is surrounded by nested cylinders: first 1 cm thick copper, then 15 cm of polyethylene veto and 10 cm of lead. The neutrons are generated isotropically within the copper.

For these sample studies, an analysis threshold on the neutron-induced nuclear recoils of 20 keV was set in the argon detector and 5 keV in the xenon and germanium detectors. Scatters were rejected as WIMP-like recoils if there were multiple nuclear scatters over threshold within the target. Figure /reffig:nuclearrecoils shows the induced nuclear recoil spectra in these simulated detector targets along with the single nuclear recoil spectra. The larger liquid noble detectors show greater reductions from all nuclear scatters to single nuclear scatters due to their size. The induced recoil spectra visibly smooth out the neutron spectra, and the differences between simulations originating with the SOURCES4A and USD are minimized when studying the single nuclear recoils of interest.

TABLE V. The differences in nuclear recoil counts over threshold simulated for different origin and target materials with SOURCES 4A and USD initial neutron spectra and yields. The percentage difference is calculated as  $(\text{SOURCES4A}-\text{USD})/[(\text{SOURCES4A}+\text{USD})/2]$ . The  $\chi^2$  per degree of freedom is calculated just for the single recoil spectra shape and excludes the normalization to total neutron yield.

Materia/Target	Chain	Recoils Diff%	Singles Diff%	$\chi^2/\text{NDF}$
Borosilicate/Ar	$^{238}\text{U}$	23	34	1.24
	$^{232}\text{Th}$	27	41	1.32
PTFE/Xe	$^{238}\text{U}$	-2	11	1.89
	$^{232}\text{Th}$	23	26	1.06
Cu/Ge	$^{238}\text{U}$	-81	-58	152
	$^{232}\text{Th}$	-16	-14	5.83

Table V provides the percentage difference between the simulated nuclear recoil counts from SOURCES4A and USD neutron spectra. The difference in counts for the borosilicate and PTFE studies can nearly all be attributed to the difference in the total neutron yields. Indeed, these count differences are generally smoothed out and reduced proportionately from the yield differences in Table IV, and a  $\chi^2$  per degree of freedom test of just the recoil spectra shapes shows reasonable agreement between both simulations.

This is not the case for the neutrons originating in copper. The total yields began with a 20% agreement, but the truncation in energy of the USD spectra causes a significant difference of up to 80% for the numbers of recoils seen above threshold. These differences are eas-

239 ily seen in the lower-left panel of Figure 4 for the  $^{238}\text{U}$   
 240 neutrons originating in Cu and recoiling in a Ge target.

241 Additional tests, that are not shown here there, vetoed  
 242 events with more than 1 keV deposited from inelastic or  
 243 capture gamma ray scatters within the target, or if a  
 244 neutron capture occurred within the veto material. Al-  
 245 though no common dopants were included in the veto  
 246 materials, most neutrons did capture within the vetoes.  
 247 The remaining elastic nuclear scatters comparisons be-  
 248 tween SOURCES and USD initial spectra were analogous  
 249 to those for the single recoils.

250 The impact upon neutron background simulations for  
 251 dark matter detectors of the difference between ( $\alpha$ , n)

252 neutron spectra calculated with SOURCES4A and the  
 253 USD webtool is primarily one of overall normalization.  
 254 The differences would lead to different background pre-  
 255 dictions prior to running an experiment, but when spec-  
 256 tral fits are made to recoils seen in a detector for multiple  
 257 scatters, high energy or high radius events, the prediction  
 258 of low energy single nuclear recoils is quite robust. How-  
 259 ever, there may be other exceptions besides copper to  
 260 these spectral considerations.

261 [RAT reference needs to be added](#)

#### 262 IV. CONCLUSION

---

263 [1] W. Wilson, R. Perry, W. Charlton, and T. Parish,  
 264 Progress in Nuclear Energy **51**, 608 (2009).  
 265 [2] D. M. Mei, C. Zhang, and A. Hime, Nucl. Instrum. Meth.  
 266 **A606**, 651 (2009), arXiv:0812.4307 [nucl-ex].  
 267 [3] E.-I. statistical model code for nuclear reaction calcula-  
 268 tion, <https://www-nds.iaea.org/empire218/manual.ps>.  
 269 [4] A. Koning, D. Rochman, S. van der Marck,  
 270 J. Kopecky, J. C. Sublet, S. Pomp, H. Sjostrand,

271 R. Forrest, E. Bauge, and H. Henriksson, TENDL-  
 272 2012: TALYS-based evaluated nuclear data library,  
 273 <ftp://ftp.nrg.eu/pub/www/talys/tendl2012/tendl2012.html>.  
 274 [5] A. Koning and D. Rochman, Nuclear Re-  
 275 search and Consultancy Group (NRG),  
 276 <http://www.talys.eu/documentation/>.  
 277 [6] “Rat (is an analysis tool) users guide,” <http://rat.readthedocs.org/en/latest/>, accessed: 2016-01-21.  
 278

FIG. 3. Radiogenic neutron spectra ( $\text{n}\cdot\text{MeV}^{-1}\cdot\text{s}^{-1}\cdot\text{cm}^{-3}$ ) calculated for 1ppb  $^{238}\text{U}$  and  $^{232}\text{Th}$  decay chains, left and right panels, respectively. The  $(\alpha, n)$  reaction contribution is shown in various commonly used materials from SOURCES4A in orange and USD in blue. From top to bottom materials are: copper, titanium, stainless steel, pyrex, borosilicate glass, polyethylene and teflon (PTFE).

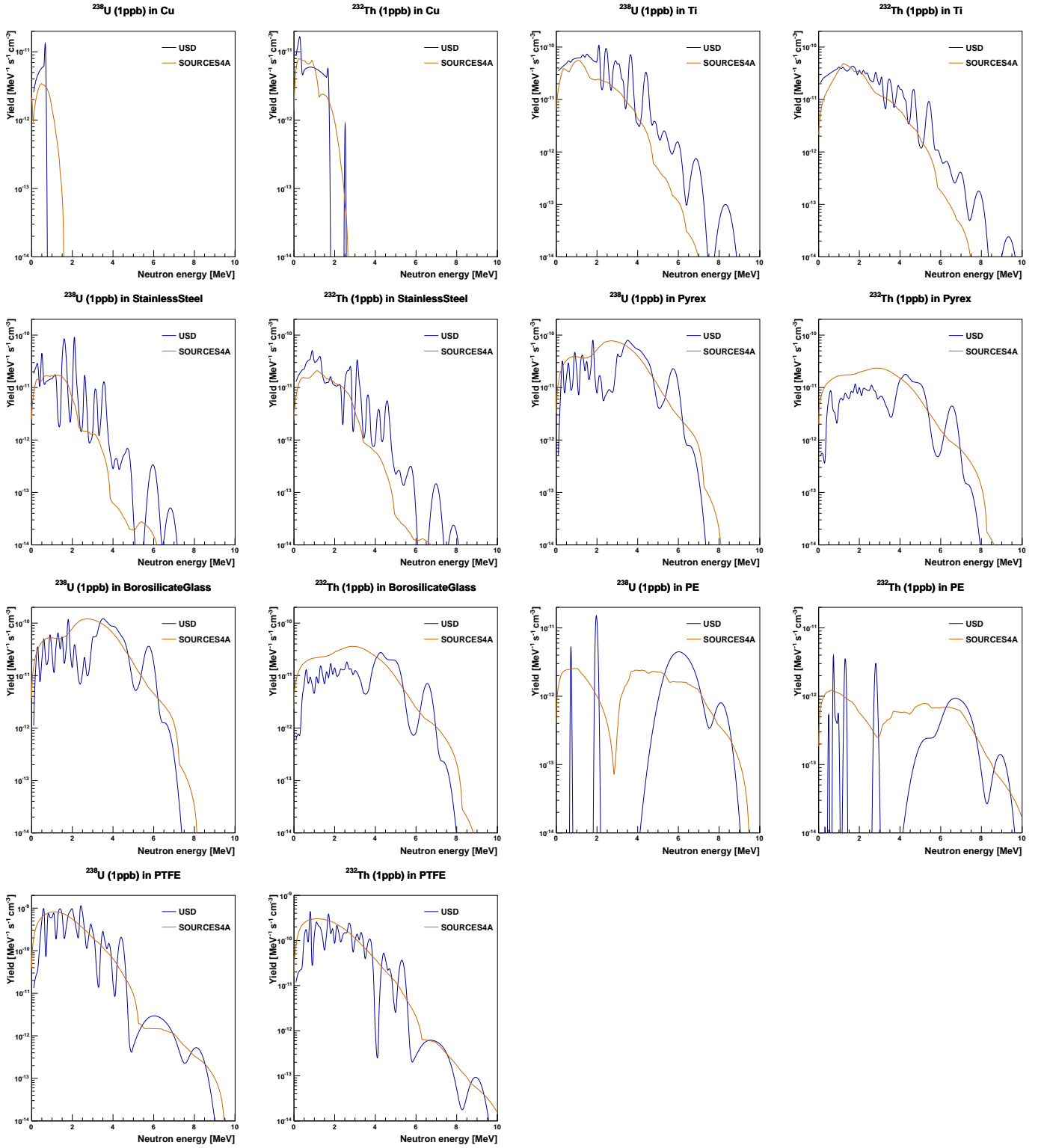


FIG. 4. Comparisons of nuclear recoils in simplified direct dark matter detector GEANT4 simulations induced from ( $\alpha$ , n) neutrons originating in detector materials. All red lines correspond to SOURCES4A initial spectra, while the USD initial spectra are plotted in blue. The solid lines are histograms of all individual nuclear recoils in the target materials, while the dashed lines are irreducible single nuclear recoils within the target. On the left are simulations for  $^{238}\text{U}$ , and  $^{232}\text{Th}$  spectra are on the right. The detectors from top to bottom are an argon target with neutrons originating in borosilicate glass, a xenon target with neutrons originating in PTFE, and a germanium target with neutrons originating in copper.

